# New Tacrine−Huperzine A Hybrids (Huprines): Highly Potent Tight-Binding Acetylcholinesterase Inhibitors of Interest for the Treatment of Alzheimer's Disease

Pelayo Camps,*,† Rachid El Achab,† Jordi Morral,† Diego Muñoz-Torrero,† Albert Badia,‡ Josep Eladi Baños,‡ Nuria María Vivas,‡ Xavier Barril,§ Modesto Orozco,|| and Francisco Javier Luque§

*Laboratori de Química Farmacèutica and Departament de Físico-Química, Facultat de Farmàcia, Universitat de Barcelona, Av. Diagonal 643, E-08028 Barcelona, Spain, Departament de Farmacologia i de Terapèutica, Facultat de Medicina, Universitat Autònoma de Barcelona, 08193-Bellaterra Barcelona, Spain, and Departament de Bioquímica, Facultat de Química, Universitat de Barcelona, Av. Martí i Franqués 1, E-08028 Barcelona, Spain*

*Received May 8, 2000*

Several new 12-amino-6,7,10,11-tetrahydro-7,11-methanocycloocta[*b*]quinoline derivatives (tacrine−huperzine A hybrids, huprines) have been synthesized and tested as acetylcholinesterase (AChE) inhibitors. All of the new compounds contain either a methyl or ethyl group at position 9 and one or two (chloro, fluoro, or methyl) substituents at positions 1, 2, or 3. Among the monosubstituted derivatives, the more active are those substituted at position 3, their activity following the order 3-chloro > 3-fluoro > 3-methyl > 3-hydrogen. For the 1,3-difluoro and 1,3-dimethyl derivatives, the effect of the substituents is roughly additive. No significant differences were observed for the inhibitory activity of 9-methyl vs 9-ethyl derivatives mono- or disubstituted at positions 1 and/or 3. The levorotatory enantiomers of these hybrid compounds are much more active (eutomers) than the dextrorotatory forms (distomers) as AChE inhibitors. Compounds *rac*-**20**, (−)-**20**, *rac*-**26**, (−)-**26**, *rac*-**30**, (−)-**30**, and *rac*-**31** showed human AChE inhibitory activities up to 28.5-fold higher than for the corresponding bovine enzyme. Also, *rac*-**19**, (−)-**20**, (−)-**30**, and *rac*-**31** were very selective for human AChE vs butyrylcholinesterase (BChE), the AChE inhibitory activities being 438−871-fold higher than for BChE. Several hybrid compounds, specially (−)-**20** and (−)-**30**, exhibited *tight-binding* character, showing higher activity after incubation of the enzyme with the inhibitor than without incubation, though the reversible nature of the enzyme−inhibitor interaction was demonstrated by dialysis. The results of the ex vivo experiments also supported the tight-binding character of compounds (−)-**20** and (−)-**30** and showed their ability to cross the blood−brain barrier. Molecular modeling simulations of the AChE−inhibitor complex provided a basis to explain the differences in inhibitory activity of these compounds.

## Introduction

Alzheimer's disease (AD) is a progressive neurodegenerative illness that affects up to 5% of people over 65 years, rising to 20% of those over 80 years.[1] Until now, most treatment strategies have been based on the cholinergic hypothesis of cognitive dysfunction of AD, which postulates that the cognitive impairment associated with AD results from a deficit of the cholinergic function in the brain.[2] Accordingly, enhancement of the central cholinergic neurotransmission has been regarded as one of the most promising approaches for treating AD patients, mainly by means of reversible acetylcholinesterase (AChE) inhibitors. The prototype for the centrally acting AChE inhibitors was tacrine[2,3] (**2**), the first drug to be approved in the United States (Cognex) for the treatment of AD. However, its severe side effects, such as hepatotoxicity and gastrointestinal upset, represent an important drawback. The results of the studies on tacrine spurred the development of other centrally acting reversible AChE inhibitors, such as the recently marketed galanthamine[4] (Nivalin), donepezil[5] (Aricept), and rivastigmine[6] (Exelon), or the natural product (−)-huperzine A[7−9] (**3**), which is currently undergoing extensive clinical trials, showing considerable promise for the palliative treatment of AD.

Bivalency is an effective strategy for improving drug potency and selectivity, when multiple recognition sites for the same substrate exist. In this sense, important efforts have been made to develop new AChE inhibitors of increased potency and selectivity, able to bind simultaneously to the catalytic and peripheral sites of AChE and not only to the catalytic site as is the case for the above-cited drugs. Several homodimeric and heterodimeric tacrine-based compounds have been recently synthesized. Among these compounds, a homodimer compound containing two units of tacrine connected by a heptamethylene chain turned out to be 149-fold more potent than tacrine inhibiting rat brain AChE.[10−12] The same strategy was used for the synthesis of some hybrid AChE inhibitors, composed of a unit of tacrine and a key fragment of huperzine A, connected by an oligomethylene chain (optimum: decamethylene), obtaining compounds up to 13-fold more potent than (−)-hu-

* To whom correspondence should be addressed. Phone: +34 +93-402-4536. Fax: +34 +93-403-5941. E-mail: camps@farmacia.far.ub.es.
† Laboratori de Química Farmacèutica, Universitat de Barcelona.
§ Departament de Físico-Química, Universitat de Barcelona.
‡ Universitat Autònoma de Barcelona.
|| Departament de Bioquímica, Universitat de Barcelona.

10.1021/jm000980y CCC: $19.00 
Published on Web 11/11/2000

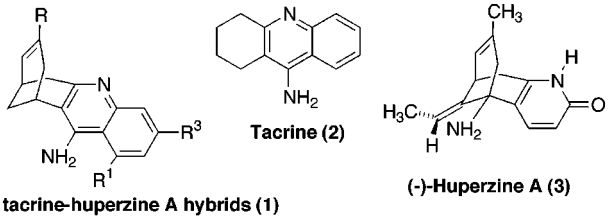


**Figure 1.** Structure of tacrine−huperzine A hybrids (huprines) and their starting models.

perzine A and 25-fold more potent than tacrine.[13] Also, some compounds, designed by dimerization of the same fragment of huperzine A, proved to be about 2-fold more potent than (−)-huperzine A and 4-fold more potent than tacrine.[14] Some galanthamine-based heterodimers were also up to 5-fold more potent than tacrine and up to 36-fold more potent than galanthamine.[15] Another bis-interacting ligand, designed by combining fragments of the structures of huperzine A and donepezil, has also been recently synthesized, although this compound showed no effective AChE inhibitory activity.[16]

Recently we have reported the synthesis, in vitro pharmacology, and molecular modeling of a series of tacrine−huperzine A hybrids (huprines) of general structure **1** (Figure 1), as AChE inhibitors of potential interest for the treatment of AD.[17−19] These compounds were originally designed in an empirical way by combination of the pharmacophores of huperzine A (carbobicyclic substructure) and tacrine (4-aminoquinoline substructure) to improve their binding to the active site of AChE. The structure of these compounds do not seem adequate to simultaneously bind to both the active sites and the peripheral sites of AChE. Several of these compounds exhibited higher AChE inhibitory activity than tacrine (**2**) and (−)-huperzine A (**3**) (Figure 1), particularly when a methyl (*rac*-**15**) or ethyl (*rac*-**21**) group was attached to position 9. Moreover, the introduction of a fluorine substituent at position 3 (*rac*-**18**) was also found to be advantageous, leading to a compound 15 times more active than tacrine in inhibiting AChE from bovine erythrocytes.[17] Likewise, the AChE inhibitory activity of the levorotatory enantiomers was roughly twice that of the racemic mixtures, while the dextrorotatory enantiomers were much less active. Molecular modeling of the interaction of these compounds with *Torpedo californica* AChE (*Tc*AChE) suggested that they behave as true tacrine−huperzine A hybrids, since the 4-aminoquinoline and bicyclo[3.3.1]-nonadiene subunits roughly occupy the same positions of the corresponding moieties in tacrine and (−)-huperzine A, respectively, as determined from their crystallographic complexes with AChE.[17,18] Later, replacement of fluorine by chlorine at position 3 (*rac*-**30**) was found to improve the inhibitory activity, leading to an inhibition constant ($K_i$) for human AChE around 30 pM, which means an affinity around 1200-fold higher than that of tacrine.[20]

Since these derivatives bind to AChE with very high affinity, it is of interest to explore in more detail the effect of these structural changes on the AChE inhibitory activity. This study reports the synthesis and pharmacological data of a new series of *rac*-huprines of general structure **1**, having R = Me or Et and one or two identical substituents (Me, F, or Cl) at different

**Scheme 1.** Synthetic Procedure for the Preparation of Huprines

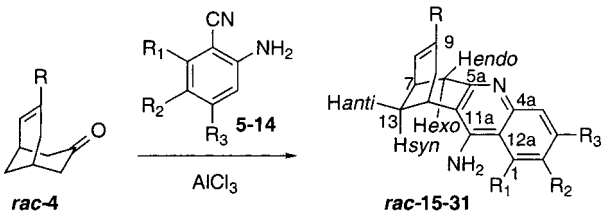


| | R |
|---|---|
| *rac*-**4a** | $CH_3$ |
| *rac*-**4b** | $CH_2CH_3$ |

| | $R_1$ | $R_2$ | $R_3$ |
|---|---|---|---|
| **5** | $CH_3$ | H | H |
| **6** | H | H | $CH_3$ |
| **7** | $CH_3$ | H | $CH_3$ |
| **8** | F | H | H |
| **9** | H | H | F |
| **10** | F | H | F |
| **11** | Cl | H | H |
| **12** | H | Cl | H |
| **13** | H | H | Cl |
| **14** | Cl | H | Cl |

| | R | $R_1$ | $R_2$ | $R_3$ |
|---|---|---|---|---|
| **15** | $CH_3$ | H | H | H |
| **16** | $CH_3$ | H | H | $CH_3$ |
| **17** | $CH_3$ | F | H | H |
| **18** | $CH_3$ | H | H | F |
| **19** | $CH_3$ | F | H | F |
| **20** | $CH_3$ | H | H | Cl |
| **21** | $CH_2CH_3$ | H | H | H |
| **22** | $CH_2CH_3$ | $CH_3$ | H | H |
| **23** | $CH_2CH_3$ | H | H | $CH_3$ |
| **24** | $CH_2CH_3$ | $CH_3$ | H | $CH_3$ |
| **25** | $CH_2CH_3$ | F | H | H |
| **26** | $CH_2CH_3$ | H | H | F |
| **27** | $CH_2CH_3$ | F | H | F |
| **28** | $CH_2CH_3$ | Cl | H | H |
| **29** | $CH_2CH_3$ | H | Cl | H |
| **30** | $CH_2CH_3$ | H | H | Cl |
| **31** | $CH_2CH_3$ | Cl | H | Cl |

positions (1, 2, 3, or 1,3) of the benzene ring. The pharmacological analysis includes: (a) inhibitory activity of bovine and human AChE and human butyrylcholinesterase (BChE), (b) neuromuscular studies focused on the ability to revert the neuromuscular blockade induced by *d*-tubocurarine, (c) time dependence and reversibility of the AChE inhibitory activity, and (d) ex vivo AChE inhibitory activity studies. Finally, molecular modeling studies have been performed to explain the differences in inhibitory activity of the more active compounds.

## Results and Discussion

**Chemistry.** The synthesis of the new compounds (*rac*-**19**, *rac*-**24**−*rac*-**29**, and *rac*-**31**) was carried out by Friedländer reaction of the known enones *rac*-**4a** and *rac*-**4b**[21] and the corresponding aminobenzonitrile **7**−**12** or **14**, under aluminum trichloride catalysis, usually in 1,2-dichloroethane as solvent under reflux. Enones *rac*-**4a** and *rac*-**4b** were easily prepared from the commercially available bicyclo[3.3.1]nonane-3,7-dione by reaction with the appropriate organomagnesium, organolithium, or organocerium reagent to give a 3-alkyl-2-oxa-1-adamantanol, which was then mesylated and submitted to a silica gel promoted fragmentation reaction. Aminobenzonitriles **7**,[22] **9**,[23] **10**,[24] **11**,[25] **12**,[26] and **14**[27] were prepared by the described procedures, while **8** is a commercial compound. Not unexpectedly on steric grounds, the yield of these reactions was low in the cases where the product contained a chlorine (*rac*-**28** and *rac*-**31**) or methyl (*rac*-**24**) substituent at position 1, despite working under more forcing conditions (100 °C, under pressure for *rac*-**28** and *rac*-**31**; 1,2-dibromoethane under reflux for *rac*-**24**). Products having a fluorine atom at position 1 (*rac*-**19**, *rac*-**25**, and *rac*-**27**) could be obtained under the standard conditions although in medium to low yields, probably due to the lower steric hindrance of the fluorine atom as compared with the chlorine atom or the methyl group.

**Table 1.** Pharmacological Data of Tacrine, (−)-Huperzine A, and the Hydrochlorides of Huprines[a]

| compd | $IC_{50}$ (nM) bovine AChE | $IC_{50}$ (nM) human AChE | $IC_{50}$ (nM) human BChE | $IC_{50}$ bovine AChE/ $IC_{50}$ human AChE | $IC_{50}$ human BChE/ $IC_{50}$ human AChE | $AI_{50}$ |
|---|---|---|---|---|---|---|
| *rac*-**15** | 65 ± 15 | *b* | 126 ± 21 | | | 176 |
| *rac*-**16** | 12.4 ± 2.3 | *b* | 449 ± 40 | | | *b* |
| *rac*-**17** | 31.4 ± 0.8 | 35.4 ± 2.4 | 543 ± 89 | 0.89 | 15.3 | 73.5 |
| *rac*-**18** | 8.5 ± 1.8 | 4.58 ± 0.19 | 197 ± 30 | 1.86 | 43.0 | 8.0 |
| *rac*-**19** | 2.43 ± 0.82 | 2.20 ± 0.38 | 963 ± 162 | 1.10 | 438 | *b* |
| *rac*-**20** | 4.23 ± 0.86 | 0.78 ± 0.02 | 236 ± 44 | 5.42 | 303 | 84.3 |
| (−)-**20** (99% ee) | 1.15 ± 0.11 | 0.32 ± 0.10 | 247 ± 18 | 3.59 | 772 | 31.6 |
| (+)-**20** (87% ee) | 36.1 ± 3.6 | 123 ± 18 | 153 ± 31 | 0.29 | 1.24 | *c* |
| *rac*-**21** | 38.5 ± 4 | *b* | 79.3 ± 9.7 | | | 84 |
| *rac*-**22** | 29.8 ± 6.2 | *b* | 512 ± 90 | | | 566 |
| *rac*-**23** | 12.0 ± 2.2 | *b* | 208 ± 27 | | | *d* |
| *rac*-**24** | 3.59 ± 0.17 | 4.96 ± 0.71 | 32.6 ± 6.5 | 0.72 | 6.57 | 166 |
| *rac*-**25** | 46.4 ± 8.5 | 29.5 ± 1.1 | 109 ± 19 | 1.57 | 3.69 | 259 |
| *rac*-**26** | 7.40 ± 1.48 | 3.79 ± 0.30 | 57.4 ± 4.6 | 1.95 | 15.1 | 38.7 |
| (−)-**26** (95% ee) | 6.73 ± 0.95 | 2.11 ± 0.58 | 32.4 ± 5.1 | 3.19 | 15.4 | *b* |
| (+)-**26** (94% ee) | 139 ± 62 | 106 ± 21 | 185 ± 15 | 1.31 | 1.75 | *b* |
| *rac*-**27** | 2.62 ± 0.70 | 1.76 ± 0.20 | 194 ± 13 | 1.49 | 110 | *b* |
| *rac*-**28** | 16.2 ± 4.4 | 11.7 ± 2.4 | 331 ± 60 | 1.38 | 28.3 | *b* |
| *rac*-**29** | 257 ± 24 | 425 ± 36 | 762 ± 13 | 0.60 | 1.79 | *d* |
| *rac*-**30** | 2.77 ± 0.75 | 0.75 ± 0.06 | 15.8 ± 2.4 | 3.69 | 21.1 | 122 |
| (−)-**30** (99% ee) | 1.30 ± 0.26 | 0.32 ± 0.09 | 159 ± 10 | 4.06 | 497 | 228 |
| (+)-**30** (97% ee) | 402 ± 36 | 23.1 ± 2.3 | 58.3 ± 5.9 | 17.4 | 2.52 | *d* |
| *rac*-**31** | 39.6 ± 11.6 | 1.39 ± 0.15 | 1210 ± 110 | 28.5 | 871 | *b* |
| (−)-huperzine A | 74.0 ± 5.5 | 260 ± 18 | >10000 | 0.28 | >38 | *b* |
| tacrine | 130 ± 10 | 205 ± 18 | 43.9 ± 17 | 0.63 | 0.21 | 71700 |

[a] Values are expressed as mean ± standard error of the mean of at least four experiments. $IC_{50}$ inhibitory concentration (nM) of AChE (from bovine or human erythrocytes) or BChE (from human serum) activity; $AI_{50}$ is the drug concentration (nM) that reaches 50% of antagonism index (AI). [b] Not determined. [c] Only 22.1% of reversion was obtained at 1 μM. [d] No reversion at 10 μM.

As previously observed, only the *anti*-regioisomers were detected in these reactions. This could be the result of a kinetic control during the cyclization step as we pointed out,[17] but it could also be the result of the acid-catalyzed isomerization of the *syn*-regioisomer under the reaction conditions, a matter which is actually being studied. Compound *rac*-**26** was separated into its enantiomers by chiral MPLC under similar conditions to those reported for other members of this series.[17,19,20]

All of the new compounds were fully characterized through their spectroscopic data (IR, $^1H$ and $^{13}C$ NMR spectra, and elemental analysis). Assignment of the $^1H$ and $^{13}C$ NMR spectra was carried out through the COSY $^1H/^1H$ and COSY $^1H/^{13}C$ spectra and by comparison with assignments previously carried out for other members of the same or related series of compounds.[17,28,29] The $^{13}C$ and $^1H$ NMR data and elemental analyses of the new compounds are collected in Tables 1−3, respectively, of the Supporting Information.

**Pharmacology.** To determine the potential interest of the new huprines for the treatment of AD, their AChE inhibitory activity was assayed by the method of Ellman et al.[30] on AChE from bovine and human erythrocytes. To establish their selectivity, their BChE inhibitory activity on human serum BChE was also assayed by the same method. For the more active compounds the time dependence of the inhibition was determined after a period of incubation of 30 min. The reversibility of the inhibition process was also studied. Moreover, the ex vivo AChE inhibitory activity in mouse brain was evaluated after treating animals with these compounds. Finally, most of them were further analyzed in a peripheral cholinergic synapse, such as the skeletal neuromuscular junction. In this analysis, the ability to reverse the *d*-tubocurarine-induced neuromuscular blockade, a well-known effect of AChE inhibitors, was tested.

Table 1 summarizes the data comparing bovine and human AChE and human BChE inhibition as well as the ratio between AChE and BChE inhibitory activities for the new huprines, and tacrine and (−)-huperzine A, as reference compounds. The reversion of the neuromuscular blockade for most of the hybrid compounds and tacrine is also shown. Most of the new compounds (*rac*-**19**, *rac*-**24**, *rac*-**26**, and *rac*-**27**) and *rac*-**20** and *rac*-**30**, whose syntheses were previously reported,[19,20] are clearly more active than tacrine and (−)-huperzine A as bovine AChE inhibitors. As previously observed in this series of compounds,[17] the levorotatory enantiomers [(−)-**20**, (−)-**26**, and (−)-**30**] are more active than the corresponding racemic mixtures, while the dextrorotatory enantiomers are clearly less potent. With the exception of *rac*-**29**, which is the sole compound substituted at position 2, the rest of compounds (*rac*-**25**, *rac*-**28**, and *rac*-**31**) are slightly more potent than (−)-huperzine A. In contrast to tacrine and (−)-huperzine A, which are less active toward human than bovine AChE, *rac*-**20**, (−)-**20**, *rac*-**30**, (−)-**30**, and *rac*-**31** are more potent toward human AChE. Regarding the BChE inhibitory activity, tacrine is 5-fold more active toward human BChE than toward human AChE, while (−)-huperzine A is highly selective for human AChE. Among the huprines, *rac*-**19**, *rac*-**20**, (−)-**20**, (−)-**30**, and *rac*-**31** showed a high selectivity for human AChE, while the rest of the new hybrid compounds showed an intermediate selectivity for this enzyme.

The results in Table 1 for the bovine AChE inhibitory activity allow us to conclude that: (a) with the exception of *rac*-**25** (1-F,9-Et), for a given substituent (Me or Et) at position 9 the monosubstituted (Cl, F, or Me) derivatives at position 1 or 3 are more active than their parent compounds [e.g., *rac*-**20** (3-Cl,9-Me), *rac*-**18** (3-F,9-Me), and *rac*-**16** (3-Me,9-Me) are 15.4-, 7.6-, and 5.2-fold more active than *rac*-**15** (3-H,9-Me), respectively, and *rac*-**30**

(3-Cl,9-Et), *rac*-**26** (3-F,9-Et), and *rac*-**23** (3-Me,9-Et) are 13.9-, 5.2-, and 3.2-fold more active than *rac*-**21** (3-H,9-Et), respectively]; (b) the AChE inhibitory activity varies in the order Cl > F > Me [e.g., *rac*-**20** (3-Cl,9-Me) is 2.0- and 2.9-fold more active than *rac*-**18** (3-F,9-Me) and *rac*-**16** (3-Me,9-Me), respectively, while *rac*-**30** (3-Cl,9-Et) is 2.7- and 4.3-fold more active than *rac*-**26** (3-F,9-Et) and *rac*-**23** (3-Me,9-Et), respectively]; (c) for a given substituent at the benzene ring, the derivative substituted at position 3 is more active than that substituted at position 1 [e.g., *rac*-**30** (3-Cl,9-Et) is 5.8-fold more active than *rac*-**28** (1-Cl,9-Et), *rac*-**26** (3-F,9-Et) is 6.3-fold more active than *rac*-**25** (1-F,9-Et), *rac*-**23** (3-Me,9-Et) is 2.5-fold more active than *rac*-**22** (1-Me,9-Et), and *rac*-**18** (3-F,9-Me) is 3.7-fold more active than *rac*-**17** (1-F,9-Me)], the activities of the 9-Et and 9-Me derivatives being very similar; (d) substitution at position 2 leads to less active compounds [e.g., *rac*-**29** (2-Cl,9-Et) is 6.7-fold less active than the parent compound *rac*-**21** (2-H,9-Et)]; (e) for the 1,3-difluoro and 1,3-dimethyl derivatives the effect of the substitutions on the AChE inhibitory activity is roughly additive; (f) in all cases, the levorotatory enantiomers are the eutomers [e.g., (−)-**20** (3-Cl,9-Me), (−)-**26** (3-F,9-Et), and (−)-**30** (3-Cl,9-Et) are 3.8-, 1.1-, and 2.1-fold more active than their racemic mixtures, while (+)-**20**, (+)-**26**, and (+)-**30** are 8.5-, 18.8-, and 145-fold less active than their racemic mixtures. These values are only indicative since no corrections were made to take into account the ee's of the enantioenriched compounds]. The above results for the racemic compounds parallel those reported by Kawakami et al.[31] for other tacrine derivatives.

The results in Table 1 also indicate that, in general, the more active compounds toward bovine AChE show an increased activity toward human AChE, showing subnanomolar $IC_{50}$ values in several cases [e.g., *rac*-**20**, (−)-**20**, *rac*-**26**, (−)-**26**, *rac*-**30**, (−)-**30**, and *rac*-**31** exhibit human AChE inhibitory activities 2−28.5-fold higher than for the bovine enzyme], whereas (−)-huperzine A and tacrine exhibit higher inhibitory activity toward bovine AChE.

Likewise, although it is not fully established that the selectivity in inhibiting AChE vs BChE results in low peripheral cholinergic effects in AD patients,[32] it is worth noting that these compounds, particularly *rac*-**19**, (−)-**20**, (−)-**30**, and *rac*-**31**, are 438−871-fold more active inhibiting human AChE than human BChE, being much more selective than tacrine (Table 1).

Several of these compounds have been submitted to neuromuscular studies. Most of the tested compounds are more potent than tacrine in reversing the neuromuscular blockade induced by *d*-tubocurarine (Table 1). The most and the least active compounds among the new tested huprines are (−)-**20** and (−)-**30**, which are 2269- and 249-fold more active than tacrine, respectively. Among all of the hybrids so far prepared, only *rac*-**18** ($AI_{50}$ = 8.0 nM)[17] is more active than (−)-**20** in reversing the neuromuscular blockade. The discrepancy observed between the AChE inhibitory potency of racemates and enantiomers and the reversion of the neuromuscular blockade was discussed in a preceding paper.[17]

Inspection of the data in Table 2 shows that the inhibitory activity is affected by incubation of the enzyme with the inhibitor before addition of substrate. Worthy of note, the 3-chloro derivatives (−)-**20** and (−)-**30** showed $IC_{50}$ values much lower after incubation of the AChE with the inhibitor for 30 min than when AChE activity was measured without previous incubation.

**Table 2.** AChE Inhibitory Activity of Several Hydrochlorides of Huprines at Different Incubation Times[a]

| compd | $IC_{50}$ (nM) | |
|---|---|---|
| | 0-min incubation | 30-min incubation |
| *rac*-**20** | 3.10 ± 1.12 | 0.64 ± 0.17[b] |
| (−)-**20** (99% ee) | 3.03 ± 0.81 | 0.0245 ± 0.0070[c] |
| *rac*-**25** | 3.20 ± 0.51 | 3.58 ± 0.24 |
| *rac*-**26** | 1.91 ± 0.88 | 0.50 ± 0.08 |
| *rac*-**30** | 3.34 ± 0.42 | 0.23 ± 0.01[b] |
| (−)-**30** (99% ee) | 2.31 ± 0.53 | 0.0674 ± 0.0128[c] |
| (+)-**30** (97% ee) | 240 ± 120 | 350 ± 140 |

[a] $IC_{50}$ is the concentration that inhibits 50% of AChE activity from bovine erythrocytes after 0- and 30-min incubation of the enzyme with the inhibitor. [b] $P < 0.05$. [c] $P < 0.01$ vs 0-min incubation (Student's *t*-test).

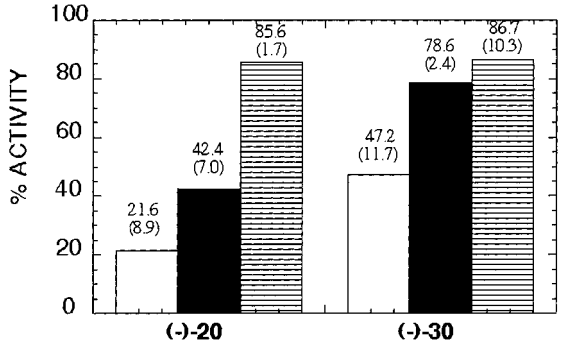


**Figure 2.** AChE activity after 30-min incubation with 25 pM (−)-**20** or (−)-**30** (white column) and after dialysis for 18 h at 4 °C (black column) or at 37 °C (striped column). Values in parentheses are confidence limits. $P < 0.01$ and $< 0.05$ for AChE activity of (−)-**20** and (−)-**30**, respectively, after dialysis at 37 °C, compared with 30-min drug incubation without dialysis.

To determine the reversibility of the inhibition process, AChE was incubated for 30 min at 25 °C with enough quantity of either (−)-**20** or (−)-**30** to give approximately 60% inhibition in each case and the samples were then dialyzed. Activity was not fully recovered after dialysis overnight at 4 °C. This fact and the high potency exhibited by these compounds indicated that they could behave as *tight-binding* inhibitors.[33] To check this possibility, enzyme−inhibitor mixtures were dialyzed at 37 °C for 18 h. This resulted in complete recovery of the activity, confirming that a reversible tight-binding inhibitory process was involved (Figure 2). The preceding results indicate that the AChE inhibitory activity is affected by the incubation time, specially for the eutomers (−)-**20** and (−)-**30**, this effect being likely due to a low dissociation constant of the corresponding AChE−inhibitor complex.[20]

The ex vivo AChE inhibitory activity in mouse brain was determined for the more active compounds. Only one dose (10 $\mu$mol $kg^{-1}$, ip) of the selected compounds was administered 20 min before the animals were sacrificed, and the percentage of AChE inhibition vs control was measured. Results in Table 3 show that huprines cross the blood−brain barrier. Both *rac*-**20** and *rac*-**30** are significantly more active than *rac*-**25** and *rac*-

**Table 3.** Ex Vivo AChE Inhibitory Activity of Several Hydrochlorides of Huprines[a]

| compd | % inhibition over control |
|---|---|
| *rac*-**20** | 59.2 ± 8.2 |
| (−)-**20** (99% ee) | 97.0 ± 0.6 |
| (+)-**20** (87% ee) | 23.4 ± 1.2 |
| *rac*-**25** | 3.6 ± 1.0 |
| *rac*-**26** | 10.4 ± 4.3 |
| *rac*-**30** | 60.3 ± 7.3 |
| (−)-**30** (99% ee) | 76.6 ± 3.8 |
| (+)-**30** (97% ee) | 4.8 ± 1.2 |
| tacrine | 0 |

[a] In all cases, 10 $\mu$mol kg$^{-1}$ was used and animals were sacrificed 20 min posttreatment. The results are the percentage of inhibition of brain AChE activity of drug-treated mice vs untreated controls. Each value is the mean ± standard error of at least six animals.

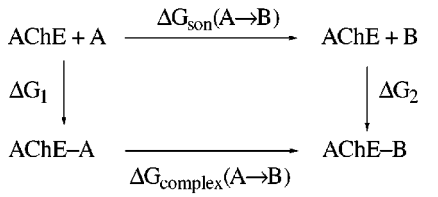


**Figure 3.** Thermodynamic cycles used in free energy calculations to determine relative binding affinities between the inhibitors.

**26** in this test. The levorotatory enantiomers are more active than the racemic mixtures, while the dextrorotatory enantiomers are much less active. In fact, the marked inhibitory activity of (−)-**20** and (−)-**30** supports the tight-binding character of these compounds. In contrast, tacrine does not show activity at the doses used, but this might be due to dissociation of the reversible enzyme–inhibitor complex owing to the necessary dilution of the tissue sample.

The preceding results point out that (−)-**20** and (−)-**30** have a set of valuable pharmacological properties (very high human AChE inhibitory activity, high human AChE vs BChE selectivity, tight-binding nature, reversibility, ability to cross the blood–brain barrier, and high activity in reversing the neuromuscular blockade induced by *d*-tubocurarine), which make them suitable candidates as potential therapeutic agents for the treatment of AD.

**Molecular Modeling Studies.** Free energy calculations were performed (Figure 3) to determine the effect of the introduction of a chlorine atom at position 3 and of the methyl → ethyl replacement at position 9 on the binding of the huprine inhibitors to AChE. These substitutions involve contacts of the drug in two distant regions of the binding pocket, and the calculations allow us to examine the additivity of those structural changes on the binding affinities. The free energy profiles for the mutations in water and in the protein (Figure 3) varied smoothly, and no discontinuities were found. The free energy differences determined in the first (equilibration) and second (collection) halves of each window were almost identical. Finally, the thermodynamic cycles for mutations 3-H,9-Me → 3-F,9-Me → 3-F,9-Et → 3-H,9-Et and 3-F,9-Me → 3-Cl,9-Me → 3-Cl,9-Et → 3-F,9-Et in water and in the protein were closed with an error lower than 0.3 kcal mol$^{-1}$. Overall, all these analyses give us confidence in the computed relative binding affinities between inhibitors.

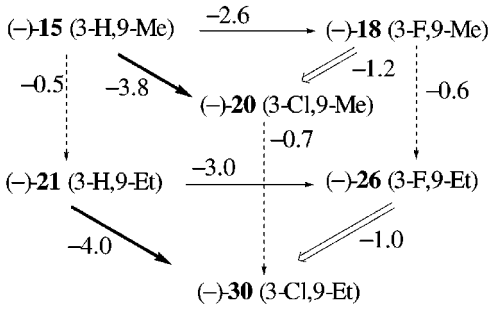


**Figure 4.** Free energy differences (kcal·mol$^{-1}$) for the binding of the (−)-enantiomer of the huprines (−)-**15** (3-H,9-Me), (−)-**18** (3-F,9-Me), (−)-**26** (3-F,9-Et), (−)-**20** (3-Cl,9-Me), and (−)-**30** (3-Cl,9-Et) to *Tc*AChE.

The predicted differences in binding free energy for conversion of the 3-F,9-Me and 3-F,9-Et compounds into their 3-chloro derivatives are given in Figure 4, which also shows the values for the corresponding Me → Et mutations. The results indicate that the effect of the substitutions at positions 3 and 9 on the binding affinity is largely additive, indicating that the active site can accommodate such structural changes without disturbing the binding. Replacement of F by Cl improves the binding to AChE by 1.0−1.2 kcal mol$^{-1}$ (Figure 4). This effect mainly arises from a better fit of the chlorine atom in the pocket formed by residues Leu333, Met436, Ile439, and Trp432, leading to an increase in the nonelectrostatic interaction relative to the fluoro derivatives. Likewise, the methyl → ethyl mutation increases the drug binding by 0.5−0.6 kcal mol$^{-1}$ (Figure 4). In this case, the effect is largely due to a better desolvation of the ethyl group. Overall, the 3-chloro derivatives are predicted to bind AChE around 3.9 kcal mol$^{-1}$ better than the parent compound, which agrees with the free energy difference of 2.2 kcal mol$^{-1}$ estimated from the experimental bovine AChE inhibitory data.[34]

A series of 1-ns molecular dynamics (MD) simulations was performed to explore the structural and energetic fluctuations of the AChE complexes with the 3-chloro derivatives. Table 4 gives the values of selected structural and energetic properties averaged from 100 structures collected during the last 0.5 ns. Inspection of Table 4 shows the lack of relevant structural alterations both in the mobile part and in the subset of residues forming the binding site. The pattern of interactions that define the proposed binding mode[17] is maintained along all the simulation for the chloro derivatives, as noted in the geometrical and energetic parameters taken from the interaction with selected residues. All of these results reinforce our confidence in the suitability of the binding mode proposed to explain the binding of huprines with AChE.

Free energy calculations were also performed to explore how the mutation Phe330 → Tyr, the corresponding residue in human AChE, may influence the affinity of the chloro derivatives. Figure 5 shows the computed free energy differences for the Phe330 → Tyr mutation in the isolated enzyme and in the AChE–drug complexes. Such a mutation is expected to stabilize around 0.3−0.4 kcal mol$^{-1}$ the binding of the inhibitors to the human enzyme relative to binding to *Tc*AChE

**Table 4.** Selected Structural and Energetic Details for the Complexes of *T. californica* and the Mutated Phe330 → Tyr AChE with the Levorotatory Enantiomers of the Parent Compound (−)-**15** and the Chloro Derivatives (−)-**20** and (−)-**30**

| | *Tc*AChE | | | Phe330 → Tyr AChE | | |
|---|---|---|---|---|---|---|
| property[a] | (−)-**15** 3-H,9-Me | (−)-**20** 3-Cl,9-Me | (−)-**30** 3-Cl,9-Et | (−)-**15** 3-H,9-Me | (−)-**20** 3-Cl,9-Me | (−)-**30** 3-Cl,9-Et |
| rmsd (all) | 0.9 (<0.1) | 0.9 (<0.1) | 0.8 (<0.1) | 1.0 (<0.1) | 0.9 (<0.1) | 0.8 (<0.1) |
| rmsd (subset) | 0.7 (<0.1) | 0.7 (<0.1) | 0.7 (<0.1) | 0.7 (<0.1) | 0.7 (<0.1) | 0.7 (<0.1) |
| *d* drug−Trp84 | 4.0 (0.5) | 4.1 (0.5) | 4.0 (0.5) | 4.1 (0.5) | 4.0 (0.5) | 4.0 (0.5) |
| α drug−Trp84 | 11.8 (4.7) | 11.8 (4.7) | 11.4 (4.5) | 12.5 (5.1) | 10.9 (4.4) | 10.7 (5.6) |
| *d* drug−Phe330(Tyr) | 3.9 (0.5) | 3.8 (0.4) | 4.0 (0.5) | 3.9 (0.5) | 3.9 (0.4) | 4.0 (0.5) |
| α drug−Phe330(Tyr) | 13.8 (7.0) | 10.4 (5.3) | 11.7 (5.8) | 13.2 (7.5) | 9.6 (6.1) | 13.6 (6.1) |
| *d* NH−OC(His440) | 2.9 (0.1) | 2.9 (0.1) | 2.9 (0.1) | 2.9 (0.1) | 2.9 (0.1) | 2.9 (0.1) |
| *d* $NH_2$−Oδ1(Asp72) | 5.0 (0.6) | 4.7 (0.4) | 4.6 (0.4) | 4.8 (0.4) | 4.7 (0.3) | 4.7 (0.3) |
| *d* $NH_2$−Oδ2(Asp72) | 6.2 (0.7) | 5.6 (0.5) | 5.5 (0.5) | 5.9 (0.5) | 5.6 (0.4) | 5.4 (0.4) |
| *d* $NH_2$−OH(Tyr330) | | | | 3.4 (0.3) | 3.5 (0.3) | 3.5 (0.3) |
| $E_{int}$ Trp84 | −10.8 (1.3) | −10.6 (1.4) | −10.0 (1.4) | −10.2 (1.1) | −10.8 (1.4) | −10.2 (1.4) |
| $E_{int}$ Phe330(Tyr) | −5.4 (0.9) | −6.7 (1.0) | −6.9 (0.9) | −6.0 (1.4) | −7.3 (1.5) | −7.7 (1.5) |
| $E_{int}$ Asp72 | −47.0 (3.9) | −50.8 (2.6) | −51.3 (2.8) | −48.5 (2.8) | −50.9 (2.5) | −51.6 (2.3) |
| $E_{int}$ His440 | −17.3 (1.1) | −18.0 (1.1) | −18.0 (1.2) | −17.5 (1.0) | −17.9 (1.2) | −18.0 (1.3) |

[a] rmsd, root-mean square deviation (Å) determined for all the heavy atoms in the mobile part (all) and for a subset of residues forming the walls of the binding site (subset); *d*, distance (Å); α, angle (deg); $E_{int}$, interaction energy (kcal $mol^{-1}$) between the drug and residues lying within the cutoff distance. Values averaged for 100 structures collected during the last 0.5 ns of MD simulations. The standard deviation is given in parentheses.

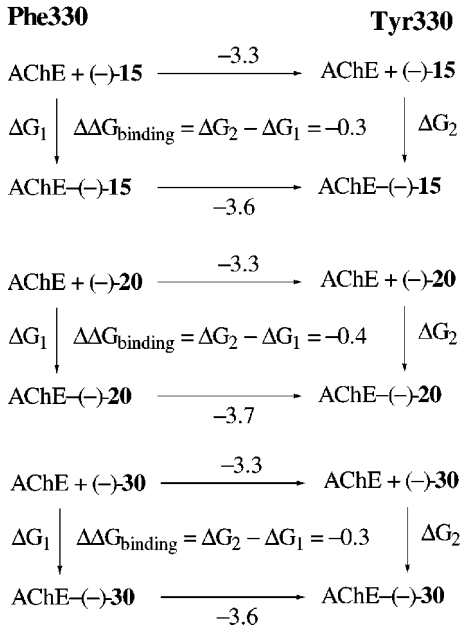


**Figure 5.** Changes in the binding free energy (kcal·$mol^{-1}$) of the (−)-enantiomer of the huprines (−)-**15** (3-H,9-Me), (−)-**20** (3-Cl,9-Me), and (−)-**30** (3-Cl,9-Et) arising from mutation of Phe330 in *Tc*AChE to the corresponding Tyr residue in the human enzyme.

(Figure 5). Accordingly, the relative binding affinities of the inhibitors for the mutated enzyme are expected to be slightly higher than the values computed for the *T. californica* enzyme. This suggests that the Phe330 → Tyr mutation does not alter remarkably the interaction pattern with the drug and particularly that the hydroxyl group does not participate directly in drug binding.

To further corroborate these conclusions, a series of 1-ns MD simulations were conducted for the Phe330 → Tyr mutated enzyme complexed with the 3-chloro derivatives. Again, the analysis of 100 structures collected during the last 0.5 ns showed no significant structural or energetic alteration, and the inhibitor remained firmly bound to the binding site of the enzyme maintaining the pattern of interactions with neighboring residues. This can be seen in Table 4, which gives selected average structural and energetic parameters for the Phe330 → Tyr AChE complexes with the parent compound and its 3-chloro derivatives. The analysis of the structures showed that the hydroxyl group has no direct interaction with the drug, since it is solvated on average by one water molecule lying at around 3 Å along all the simulations. Indeed, results in Table 4 show that the interaction of the inhibitor with Tyr330 is slightly more favorable (around 0.7 kcal $mol^{-1}$) than with Phe330, as noted in the results of the free energy calculations (Figure 5).

In summary, the whole of results reflects the changes in the available experimental data originated by attachment of chlorine atoms at position 3 of the huprine derivatives. In all cases the enzyme−drug complex shows no relevant structural fluctuations and the pattern of interactions is fully preserved along the simulation. Indeed, the results determined for the Phe330 → Tyr mutation indicate that this change is expected to enhance slightly the binding to the enzyme. Overall, the results support the validity of the putative binding model for huprines to AChE, which gives a valuable basis to continue our current efforts in developing AChE inhibitors with improved inhibitory activity.

## Conclusion

The AChE inhibitory activity of a series of huprines of general structure **1**, having an Et or Me group at position 9, increases on substitution at positions 1 and/or 3 (benzene ring) with Cl, F, and/or Me substituents. The more active derivatives are those substituted at position 3 with a Cl atom (**20** and **30**). In the whole series, the levorotatory enantiomers are much more active than the dextrorotatory enantiomers. Several huprines and especially (−)-**20** and (−)-**30** proved to be more active toward human than bovine AChE. They are quite selective inhibiting human AChE vs human BChE, which may be indicative of reduced peripheral effects. Also, the tight-binding nature of the above two inhibitors has been evidenced by the dependence of their activity on the time of incubation of the enzyme with the inhibitor, although both of them have shown to be reversible inhibitors able to cross the blood−brain

barrier. Moreover, all of these huprines proved to be much more active than tacrine in reversing the neuromuscular blockade induced by *d*-tubocurarine. The molecular modeling studies of the complexes of (−)-huprines having a chlorine atom at position 3 and an Et group at position 9 with *Tc*AChE and the Phe330 → Tyr mutated enzyme using the previously proposed model[17,18] are in reasonable agreement with the experimental activity values. Despite the agreement with the experimental data, the definite validation of the binding model has to await a 3D X-ray structure of the complex.

Altogether, huprines (−)-**20** and (−)-**30** are very potent human AChE inhibitors. In conjunction with their AChE vs BChE selectivity, tight-binding but reversible character, and ability to reverse the neuromuscular blockade induced by *d*-tubocurarine, these findings make them very interesting candidates for further studies in connection with their possible use in the treatment of AD.

## Experimental Section

**Chemistry. General Methods.** Melting points were determined in open capillary tubes with a MFB 595010M Gallenkamp melting point apparatus. $^1$H NMR spectra were recorded at 500 MHz on a Varian VXR 500 spectrometer, and $^{13}$C NMR spectra were recorded at 75.4 MHz on a Varian Gemini 300 spectrometer. The chemical shifts are reported in ppm ($\delta$ scale) relative to internal TMS, and coupling constants are reported in hertz (Hz). COSY $^1$H/$^1$H experiments were performed using standard procedures, while COSY $^1$H/$^{13}$C were performed using the HMQC sequence with an indirect detection probe. For the $^{13}$C and $^1$H NMR data of the new huprines, see Tables 1 and 2, respectively, of Supporting Information. IR spectra were run on a FT/IR Perkin-Elmer model 1600 spectrophotometer. Absorption values are expressed as wavenumbers (cm$^{-1}$). Optical rotations were measured on a Perkin-Elmer model 241 polarimeter. The specific rotation has not been corrected for the presence of solvent of crystallization. Chiral HPLC analyses were performed on a Waters model 600 liquid chromatograph provided with a Waters model 486 variable $\lambda$ detector, using a CHIRALCEL OD-H column (25 × 0.46 cm) containing the chiral stationary phase cellulose tris-(3,5-dimethylphenylcarbamate). Conditions A: mixture of hexane/EtOH/Et$_2$NH in the ratio of 90:10:0.1 as eluent, flow 0.20 mL min$^{-1}$, $\lambda$ = 235 nm. Chiral medium-pressure liquid chromatography (chiral MPLC) separations were carried out on an equipment which consisted of a pump (Büchi 688), a variable $\lambda$ UV detector (Büchi), and a column (25 × 2.5 cm) containing microcrystalline cellulose triacetate (15−25 $\mu$m) as the chiral stationary phase. Column chromatography was performed on silica gel 60 AC.C. (70−200 mesh, SDS, ref 2100027). For the TLC, aluminum-backed sheets with silica gel 60 $F_{254}$ (Merck, ref 1.05554) were used. $AlCl_3$ was purchased from Aldrich. Analytical grade solvents were used for recrystallizations, while pure for synthesis solvents were used in extractions and column chromatography. Pure-for-synthesis 1,2-dichloroethane and 1,2-dibromoethane were also used. Aminobenzonitrile **8** was purchased from ABCR while **7**, **9**−**12**, and **14** were prepared according to literature procedures. Elemental analyses were carried out at the Mycroanalysis Service of the Centro de Investigación y Desarrollo, C.I.D., Barcelona, Spain, and are within ±0.4% of the theoretical values.

**General Procedure for the Preparation of *rac*-Huprines from Enones *rac*-4 and 2-Aminobenzonitriles 7−12 and 14.** To a suspension of anhydrous $AlCl_3$ (1.8 mmol) and 2-aminobenzonitrile **7**−**12** or **14** (1.3 mmol) in 1,2-dichloroethane (2 mL) was added a solution of enone *rac*-**4a** or *rac*-**4b** (1 mmol) in 1,2-dichloroethane (10 mL) dropwise. The reaction mixture was stirred under reflux for 7 h, allowed to cool to room temperature, diluted with water (8 mL) and THF (12 mL), made basic by addition of 5 N NaOH, and stirred at room temperature for 30 min. The organic solvents were removed under reduced pressure, and the residue was filtered. The solid residue was submitted to column chromatography [silica gel (13 g), hexane/AcOEt/MeOH mixtures] to give the *rac*-huprine. A solution of this compound in MeOH was treated with a solution of HCl in $Et_2O$ or in MeOH (3 equiv), and the solvent was evaporated to give the corresponding hydrochloride, which was recrystallized.

***rac*-12-Amino-1,3-difluoro-6,7,10,11-tetrahydro-9-methyl-7,11-methanocycloocta[*b*]quinoline Hydrochloride (*rac*-19·HCl).** This compound was prepared according to the procedure described above, but using 1.1 equiv of $AlCl_3$ and 0.8 equiv of aminobenzonitrile **10**. The alkaline mixture was concentrated in vacuo, diluted with water and extracted with AcOEt. The combined organic extracts were dried over $Na_2SO_4$ and evaporated under reduced pressure to give a solid residue which was submitted to column chromatography. On elution with hexane/AcOEt 80:20, slightly impure *rac*-**19** (110 mg) was obtained as a yellow solid which was again submitted to column chromatography [silica gel (11 g), hexane/$Et_2O$, gradient elution]. On elution with hexane/$Et_2O$ 75:25, pure *rac*-**19** (60 mg, 30% yield) was isolated. Subsequent treatment with a solution of HCl (0.38 N solution in $Et_2O$, 3 equiv), evaporation and recrystallization of the resulting solid from acetonitrile afforded *rac*-**19**·HCl·1/2$H_2O$ (13% overall yield): mp > 300 °C dec; IR 3500−2500 (max at 3509, 3289, 3170, 2917, 2882, 2859, 2704, 2681) (CH, NH, NH$^+$), 1650 and 1594 (ar-C−C and ar-C−N). Anal. ($C_{17}H_{16}F_2N_2$·HCl·1/2$H_2O$) C, H, N.

***rac*-12-Amino-9-ethyl-6,7,10,11-tetrahydro-1,3-dimethyl-7,11-methanocycloocta[*b*]quinoline Hydrochloride (*rac*-24·HCl).** This compound was prepared according to the procedure described above, but using 1,2-dibromoethane as solvent and a reaction time of 21 h. On elution with AcOEt/MeOH 90:10, *rac*-**24** (0.90 g, 24% yield) was isolated. Subsequent treatment with a solution of HCl (0.37 N solution in MeOH, 3 equiv), evaporation and recrystallization of the resulting solid from MeOH afforded *rac*-**24**·HCl·$H_2O$ (11% overall yield): mp 316−318 °C dec; IR 3500−2500 (max at 3401, 3306, 3209, 3040, 2869) (CH, NH, NH$^+$), 1647 and 1590 (ar-C−C and ar-C−N). Anal. ($C_{20}H_{24}N_2$·HCl·$H_2O$) C, H, N, Cl.

***rac*-12-Amino-9-ethyl-1-fluoro-6,7,10,11-tetrahydro-7,11-methanocycloocta[*b*]quinoline Hydrochloride (*rac*-25·HCl).** This compound was prepared according to the procedure described above. On elution with hexane/AcOEt 30:70, *rac*-**25** (430 mg, 29% yield) was isolated. Subsequent treatment with a solution of HCl (0.37 N solution in MeOH, 3 equiv), evaporation, and recrystallization of the resulting solid from acetonitrile/MeOH 10:1, afforded *rac*-**25**·HCl·3/2$H_2O$ (13% overall yield): mp 160−162 °C; IR 3600−2400 (max at 3334, 3208, 3070, 2963, 2931, 2899, 2835) (CH, NH, NH$^+$), 1638 and 1594 (ar-C−C and ar-C−N). Anal. ($C_{18}H_{19}FN_2$·HCl·3/2$H_2O$) C, H, N, Cl.

***rac*-12-Amino-9-ethyl-3-fluoro-6,7,10,11-tetrahydro-7,11-methanocycloocta[*b*]quinoline Hydrochloride (*rac*-26·HCl).** This compound was prepared according to the procedure described above. On elution with hexane/AcOEt 30:70, *rac*-**26** (0.55 g, 40% yield) was isolated. Subsequent treatment with a solution of HCl (0.55 N solution in MeOH, 3 equiv), evaporation, and recrystallization of the resulting solid from MeOH/$H_2O$ 1:6, afforded *rac*-**26**·HCl·1/2$H_2O$ (28% overall yield): mp 202−206 °C dec; IR 3500−2500 (max at 3332, 3180, 2929, 2822, 2696) (CH, NH, NH$^+$), 1640 and 1591 (ar-C−C and ar-C−N). Anal. ($C_{18}H_{19}FN_2$·HCl·1/2$H_2O$) C, H, N, Cl.

**Preparative Resolution of *rac*-26 by Chiral MPLC: (+)-(7*R*,11*R*)-26 and (−)-(7*S*,11*S*)-26.** The chromatographic resolution of *rac*-**26** was carried out by using the above-described MPLC equipment, pretreating the chiral stationary phase with a 0.1% solution of $Et_3N$ in EtOH. The sample of *rac*-**26** (1.00 g) was introduced as free base in 2 portions (1 × 100 mg + 1 × 900 mg) using 96% EtOH (2 mL.min$^{-1}$) as the sole eluent and solvent. The chromatographic fractions (5 mL) were analyzed by chiral HPLC under conditions A [(−)-**26**, $t_R$ = 28.66 min, $k'_1$ = 0.81; (+)-**26**, $t_R$ = 32.19 min, $k'_2$ = 1.03, $\alpha$

= 1.27, res. = 1.57] and combined conveniently. In this way, (−)-**26** (235 mg, 95% ee) and (+)-**26** (200 mg, 94% ee) were obtained. The remaining product consisted of mixtures of both enantiomers with lower ee's.

A solution of (−)-**26** (235 mg, 95% ee) in MeOH (10 mL) was treated with excess 0.77 N HCl in $Et_2O$ (10 mL), and the organic solvents were removed under reduced pressure. The residue (255 mg) was recrystallized from AcOEt/MeOH 3:1 (10 mL) to afford (−)-**26**·HCl·5/4$H_2O$ {120 mg, $[\alpha]^{20}_D = -280$ (*c* = 1.00, MeOH), 95% ee by chiral HPLC on the liberated base}: mp 190−195 °C dec; IR 3500−2500 (max at 3354, 3184, 2930, 2826, 2683) (CH, NH, $NH^+$), 1654 and 1586 (ar-C−C and ar-C−N). Anal. ($C_{18}H_{19}FN_2$·HCl·5/4$H_2O$) C, H, N.

Similarly, from (+)-**26** (200 mg, 94% ee), (+)-**26**·HCl·5/4$H_2O$ {100 mg, $[\alpha]^{20}_D = +283$ (*c* = 1.00, MeOH), 94% ee by chiral HPLC on the liberated base} was obtained: mp 230−235 °C dec; IR 3500−2500 (max at 3336, 3190, 2970, 2930, 2837, 2697) (CH, NH, $NH^+$), 1639 and 1591 (ar-C−C and ar-C−N). Anal. ($C_{18}H_{19}FN_2$·HCl·5/4$H_2O$) C, H, N.

***rac*-12-Amino-9-ethyl-1,3-difluoro-6,7,10,11-tetrahydro-7,11-methanocycloocta[*b*]quinoline Hydrochloride (*rac*-27·HCl).** This compound was prepared as described for *rac*-**19**. On elution with hexane/AcOEt 70:30, *rac*-**27** (230 mg, 59% yield) was isolated. Subsequent treatment with a solution of HCl (0.38 N solution in $Et_2O$, 3 equiv), evaporation and recrystallization of the resulting solid from acetonitrile/MeOH 10:1 afforded *rac*-**27**·HCl·1/3$H_2O$ (38% overall yield): mp 270−271 °C dec; IR 3600−2300 (max at 3498, 3291, 3143, 3073, 3028, 2961, 2902, 2829, 2672) (CH, NH, $NH^+$), 1640 and 1597 (ar-C−C and ar-C−N). Anal. ($C_{18}H_{18}F_2N_2$·HCl·1/3$H_2O$) C, H, N, Cl.

***rac*-12-Amino-1-chloro-9-ethyl-6,7,10,11-tetrahydro-7,11-methanocycloocta[*b*]quinoline Hydrochloride (*rac*-28·HCl).** This compound was prepared according to the procedure described above, but heating the reaction mixture in a pressure flask at 100 °C for 7 h. On elution with hexane/AcOEt 20:80, *rac*-**28** (200 mg, 22% yield) was isolated. Subsequent treatment with a solution of HCl (0.77 N solution in $Et_2O$, 3 equiv), evaporation and recrystallization of the resulting solid from AcOEt/MeOH 4:1 afforded almost pure *rac*-**28**·HCl (130 mg), which was recrystallized under the same conditions to give pure *rac*-**28**·HCl·1/2$H_2O$ (7% overall yield): mp 212−215 °C; IR 3500−2500 (max at 3453, 3319, 3203, 3063, 3029, 2959, 2887, 2862) (CH, NH, $NH^+$), 1628 and 1580 (ar-C−C and ar-C−N). Anal. ($C_{18}H_{19}ClN_2$·HCl·1/2$H_2O$) C, H, N, Cl.

***rac*-12-Amino-2-chloro-9-ethyl-6,7,10,11-tetrahydro-7,11-methanocycloocta[*b*]quinoline Hydrochloride (*rac*-29·HCl).** This compound was prepared according to the procedure described above. On elution with hexane/AcOEt 40:60, *rac*-**29** (2.08 g, 58% yield) was isolated. Subsequent treatment with a solution of HCl (0.55 N solution in $Et_2O$, 3 equiv), evaporation and recrystallization of the resulting solid from AcOEt/MeOH 1:10 afforded pure *rac*-**29**·HCl (30% overall yield): mp 339−340 °C dec; IR 3500−2000 (max at 3320, 3262, 3144, 3071, 3024, 2964, 2929, 2881, 2793, 2679) (CH, NH, $NH^+$), 1667 and 1578 (ar-C−C and ar-C−N). Anal. ($C_{18}H_{19}ClN_2$·HCl) C, H, N, Cl.

***rac*-12-Amino-1,3-dichloro-9-ethyl-6,7,10,11-tetrahydro-7,11-methanocycloocta[*b*]quinoline Hydrochloride (*rac*-31·HCl).** This compound was prepared according to the procedure described above, but heating the reaction mixture in a pressure flask at 100 °C for 7 h. On elution with hexane/AcOEt 70:30, *rac*-**31** (110 mg, 15% yield) was isolated. Subsequent treatment with a solution of HCl (0.55 N solution in $Et_2O$, 3 equiv), evaporation and recrystallization of the resulting solid from AcOEt/MeOH 5:1 afforded impure *rac*-**31**·HCl (31 mg), which was recrystallized from acetonitrile to give pure *rac*-**31**·HCl·$H_2O$ (2% overall yield): mp > 300 °C dec; IR 3600−2200 (max at 3447, 3315, 3197, 3047, 2924, 2856, 2714, 2304) (CH, NH, $NH^+$), 1627 and 1578 (ar-C−C and ar-C−N). Anal. ($C_{18}H_{18}Cl_2N_2$·HCl·$H_2O$) C, H, N.

**Biochemical Studies.** AChE inhibitory activity was evaluated spectrophotometrically at 25 °C by the method of Ellman,[30] using AChE from bovine erythrocytes and acetylthiocholine iodide (0.53 mM) as substrate. The reaction took place in a final volume of 3 mL of 0.1 M phosphate-buffered solution pH 8.0, containing 0.025 units of AChE and 333 $\mu$M 5,5′-dithiobis(2-nitrobenzoic acid) (DTNB) solution used to produce the yellow anion of 5-thio-2-nitrobenzoic acid. Inhibition curves with different derivatives were performed in triplicate by incubating with at least 12 concentrations of inhibitor for 15 min. One triplicate sample without inhibitor was always present to yield the 100% of AChE activity. The reaction was stopped by the addition of 100 $\mu$L 1 mM eserine, and the color production was measured at 412 nm. BChE inhibitory activity determinations were carried out similarly, using 0.035 unit of human serum BChE and 0.56 mM butyrylthiocholine, instead of AChE and acetylthiocholine, in a final volume of 1 mL.

The drug concentration producing 50% of AChE or BChE activity inhibition ($IC_{50}$) was calculated by nonlinear regression. Results are expressed as mean ± SEM of at least 4 experiments performed in triplicate. DTNB, acetylthiocholine, butyrylthiocholine, and the enzymes were purchased from Sigma and eserine from Fluka.

**Time Dependence and Reversibility of Bovine AChE Inhibitory Activity.** The time dependence of the inhibitory process was determined for several of the more active compounds with at least 12 increasing inhibitor concentrations after an incubation period of 30 min. After this time the AChE inhibitory activity was assayed by the method of Ellman.[30] In this set of experiments, the appearance of product was monitored at 412 nm in a Perkin-Elmer Lambda 2 spectrophotometer equipped with an automatic six-cell changer, in the absence and presence of different inhibitor concentrations. The final incubation volume was 1 mL. The changes in absorbance/min (the slope) were calculated.

The reversibility of the inhibition process was assayed by dialysis (Visking dialysis tubing, exclusion limit 8 000−15 000 Da; Serva Feinbiochemica GmbH & Co.). The enzyme (0.6 unit) was incubated with 25 pM of each inhibitor [(−)-**20** and (−)-**30**] in a total volume of 6 mL of phosphate buffer. After 30-min incubation at 25 °C, the reaction was stopped by chilling it in an ice bath, and the remaining activity was measured in 250 mL of the mixture toward 100 mL of acetylthiocholine as substrate. The samples were then dialyzed against 1000 vol of buffer at 4 °C and at 37 °C for 18 h, and the remaining activity was again measured. Controls were taken through the same procedure in the absence of inhibitor.

**Ex Vivo AChE Inhibitory Activity.** Groups of 6 OF1 mice were treated with each compound at 10 mmol $kg^{-1}$ ip. The animals were sacrificed 20 min later and brains quickly removed and frozen on dry ice. Residual AChE activities were determined as previously described by the method of Ellman using brain homogenate preparations as a source of the enzyme. Percent of inhibitions was calculated by comparing AChE activity in brain of drug-treated mice with activity from untreated controls.

**Neuromuscular Studies.** Right and left phrenic nerve-hemidiaphragms removed from male Sprague−Dawley rats (250−300 g) were used. Details of the experimental procedures have been previously described.[35] Briefly, rats were lightly anesthetized with ether and decapitated. After quick dissection, each phrenic-hemidiaphragm preparation was suspended in organ baths of 75-mL volume with Krebs-Henseleit solution of the following composition (mM): NaCl 118, KCl 4.7, $CaCl_2$ 2.5, $KH_2PO_4$ 1.2, $NaHCO_3$ 25, and glucose 11.1. The preparation was bubbled with 5% $CO_2$ in oxygen and the temperature was maintained at 25 ± 1 °C. Effects of AChE inhibitors on neuromuscular junction were assessed as the ability of reversing the partial blockade induced by *d*-tubocurarine in indirectly elicited twitch responses. The twitches were obtained by stimulating the phrenic nerve with square pulses of 0.5-ms duration at 0.2 Hz and a supramaximal voltage (30−40 V). Neuromuscular blockade was obtained with the addition of *d*-tubocurarine (1−1.5 $\mu$M). Drugs were added when a reduction of twitch response to 70−80% control values was

achieved. The effect of each drug was evaluated after 15 min of exposure. To avoid the possible carry-over effects, only one concentration of inhibitor was tested on each preparation. Several drug concentrations were evaluated for each AChE inhibitor. To quantify the reversal effect of each drug, the antagonism index (AI or % of antagonism)[36] was determined for each concentration and the $AI_{50}$ (drug concentration that gives a 50% value of AI) was calculated by nonlinear regression. *d*-Tubocurarine was purchased from Sigma.

**Molecular Modeling: Methods**. The simulation system was based on the structure of the complex between *Tc*AChE complexed with the hybrid compounds (−)-**18** (3-fluoro-9-methyl-substituted) and (−)-**26** (3-fluoro-9-ethyl-substituted). This structure has been obtained from molecular modeling studies,[18] and its definite validation must await a 3D X-ray structure of the complex. However, the results obtained up to now agree with the available experimental evidence. The enzyme was modeled in its physiological active form with neutral His440 and deprotonated Glu327, which together with Ser200 form the catalytic triad. The standard ionization state at neutral pH was considered for the rest of ionizable residues with the exception of Asp392 and Glu443, which were neutral, and His471, which was protonated, according to previous numerical titration studies.[37] The geometry of the chloro derivatives (−)-**20** and (−)-**30** was fully optimized at the Hartree−Fock level with the 6-31G(d)[38] basis set using the Gaussian-94 program.[39] According to the $pK_a = 8.9$, measured for (−)-**30**,[20] which must be very similar to those of the other huprines of this work, the protonated species of the hybrid compounds was considered in calculations.

Free energy calculations were performed to predict the relative binding affinities of the hybrid 3-chloro derivatives. To this end, we investigated the effect of the changes fluorine → chlorine at position 3 and methyl → ethyl at position 9 on the binding free energy. Indeed, we examined the effect of mutating Phe330 in *Tc*AChE to Tyr, which is the corresponding residue in human AChE, on the binding affinities of the 3-chloro derivatives. Such a mutation is the only relevant difference concerning the residues directly involved in the binding pocket between *T. californica* and human enzymes. This simulation allows us to determine which changes in the binding affinity can be due to the use of the protein structure of a different organism.

Free energy calculations were performed using thermodynamic integration (TI) coupled to molecular dynamics (MD) for sampling of the AChE−drug configurational space following the standard algorithm implemented in AMBER-5. The starting structures in TI-MD calculations were the equilibrated AChE−drug complexes for the 3-fluoro derivatives determined in our previous study,[18] which consist of the protein, the inhibitor, and a cap of 670 TIP3P[40] water molecules centered at the inhibitor. Though the use of a cap of water molecules is an approximate treatment, we adopted it in order to enable comparison of the TI-MD results for chlorine derivatives with those previously reported for related compounds.[18] The system was partitioned into a mobile and a rigid region. The former included the inhibitor, all the protein residues containing at least one atom within 14 Å from the inhibitor, and all the water molecules, while the rest of atoms defined the rigid part. Nonbonded intramolecular contributions were included in evaluating free energy differences.[41] The mutation between inhibitors in water and in the enzyme was performed using 41 windows, each window consisting of 5 ps for equilibration and 5 ps for averaging, leading to a total of 410 ps for each simulation. Test calculations performed using a 820-ps simulation predicted no relevant differences in the computed relative binding affinities due to the use of larger trajectories.

The AMBER-95 all-atom force field[42] was used for the protein and water molecules. Following the AMBER parametrization procedure, the charge distribution of the drug was determined from fitting to the HF/6-31G(d) electrostatic potential using the RESP[43] procedure, and the van der Waals parameters were taken from those defined for related atoms in the force-field. The van der Waals parameters for chlorine ($\epsilon = 0.3$ kcal mol$^{-1}$; $r^* = 1.95$ Å) were adopted from the values in the OPLS force field.[44] SHAKE[45] was used to maintain all the bonds at their equilibrium distances, which allowed to use an integration time step of 2 fs. A cutoff of 11 Å was used for nonbonded interactions. Calculations were performed using the AMBER5 computer program.[46]

To analyze the structural and energetic features of the interaction between the drugs and the *T. californica* or mutated enzyme, a series of 1-ns MD simulations were performed using the same technical features already noted and the final structures obtained from the TI-MD calculations. The trajectory was stored every 1 ps for subsequent analysis of complexes.

**Acknowledgment.** Fellowships from Comissió Interdepartamental de Recerca i Innovació Tecnològica (CIRIT) of the Generalitat de Catalunya to J. Morral, from Agencia Española de Cooperación Internacional (Instituto de Cooperación con el Mundo Arabe, Mediterráneo y Países en Desarrollo) to R. El Achab, and from Ministerio de Educación y Cultura to X. Barril and financial support from the Comisión Interministerial de Ciencia y Tecnología (CICYT) (Programa Nacional de Tecnologías de los Procesos Químicos, Project QUI96-0828, and Programa Nacional de Salud y Farmacia, Project SAF99-0088), Fundació "La Marató de TV3" (Project 3004/97), Dirección General de Investigación Científica y Técnica (Projects PB97-0908 and PB98-1222), Comissionat per a Universitats i Recerca of the Generalitat de Catalunya (Project 1999-SGR-00080), and Medichem, S.A. are gratefully acknowledged. We also thank the Centre de Supercomputació de Catalunya (CESCA) for computational facilities, the Serveis Científico-Tècnics of the University of Barcelona and particularly Dr. A. Linares for recording the NMR spectra and Ms. P. Domènech from the Centro de Investigación y Desarrollo (C.I.D.) of Barcelona for carrying out the elemental analyses. We are indebted to Prof. Dr. A. Kozikowski (GICCS, Georgetown University, Washington, D.C.) for a generous gift of (−)-huperzine A.

**Supporting Information Available:** Tables of $^{13}C$ and $^{1}H$ NMR data of the hydrochlorides of *rac*-**19**, *rac*-**24**−*rac*-**29**, and *rac*-**31** (Tables 1 and 2), elemental analyses of all new compounds (Table 3), and bonded and nonbonded parameters for the chlorine atom in the huprines (−)-**20** and (−)-**30** (Table 4). This material is available free of charge via the Internet at http://pubs.acs.org.

## References

(1) Launer, L. J.; Fratiglioni, L.; Andersen, K.; Breteler, M. M. B.; Copeland, R. J. M.; Dartigues, J.-F.; Lobo, A.; Martinez-Lage, J.; Soininen, H.; Hofman, A. Regional Differences in the Incidence of Dementia in Europe-EURODEM Collaborative Analysis. In *Alzheimer's Disease and Related Disorders: Etiology, Pathogenesis and Therapeutics*; Iqbal, K., Swaab, D. F., Winblad, B., Wisniewski, H. M., Eds.; John Wiley & Sons: New York, 1999; pp 9−15.

(2) Gualtieri, F.; Deu, S.; Manetti, D.; Romanelli, M. N. The Medicinal Chemistry of Alzheimer and Alzheimer-like Diseases with Emphasis on the Cholinergic Hypothesis. *Farmacologie* **1995**, *50*, 489−503.

(3) Davis, K. L.; Powchik, P. Tacrine. *Lancet* **1995**, *345*, 625−630.

(4) Rainer, M. Galanthamine in Alzheimer's Disease. A New Alternative to Tacrine? *CNS Drugs* **1997**, *7*, 89−97.

(5) Sugimoto, H.; Iimura, Y.; Yamanishi, Y.; Yamatsu, K. Synthesis and Structure−Activity Relationships of Acetylcholinesterase Inhibitors: 1-Benzyl-4-[(5,6-dimethoxy-1-oxoindan-2-yl)methyl]-piperidine Hydrochloride and Related Compounds. *J. Med. Chem.* **1995**, *38*, 4821−4829.

(6) Prous, J.; Rabasseda, X.; Castañer, J. SDZ-ENA-713 Cognition Enhancer Acetylcholinesterase Inhibitor. *Drugs Future* **1996**, *19*, 656−658.

(7) Kozikowsky, A. P.; Campiani, G.; Sun, L. Q.; Wang, S.; Saxena, A.; Doctor, B. P. Identification of a More Potent Analogue of the Naturally Ocurring Alkaloid Huperzine A. Predictive Molecular Modeling of its Interaction with AChE. *J. Am. Chem. Soc.* **1996**, *118*, 11357−11362.
(8) Kozikowsky, A. P.; Tückmantel, W. Chemistry, Pharmacology, and Clinical Efficacy of the Chinese Nootropic Agent Huperzine A. *Acc. Chem. Res.* **1999**, *32*, 641−650.
(9) Bai, D. L.; Tang, X. C.; He, X. C. Huperzine A, a Potential Therapeutic Agent for Treatment of Alzheimer's Disease. *Curr. Med. Chem.* **2000**, *7*, 355−374.
(10) Pang, Y.-P.; Quiram, P.; Jelacic, T.; Hong, F.; Brimijoin, S. Highly Potent, Selective, and Low Cost Bis-Tetrahydroaminacrine Inhibitors of Acetylcholinesterase. *J. Biol. Chem.* **1996**, *271*, 23646−23649.
(11) Carlier, P. R.; Han, Y. F.; Chow, E. S.-H.; Li, C. P.-L.; Wang, H.; Lieu, T. X.; Wong, H. S.; Pang, Y.-P. Evaluation of Short-tether Bis-THA AChE Inhibitors. A Further Test of the Dual Binding Site Hypothesis. *Bioorg. Med. Chem.* **1999**, *7*, 351−357.
(12) Carlier, P. R.; Chow, E. S.-H.; Han, Y.; Liu, J.; El Yazal, J.; Pang, Y.-P. Heterodimeric Tacrine-Based Acetylcholinesterase Inhibitors: Investigating Ligand-Peripheral Site Interactions. *J. Med. Chem.* **1999**, *42*, 4225−4231.
(13) Carlier, P. R.; Du, D.-M.; Han, Y.; Liu, J.; Pang, Y.-P. Potent, Easily Synthesized Huperzine A-Tacrine Hybrid Acetylcholinesterase Inhibitors. *Bioorg. Med. Chem. Lett.* **1999**, *9*, 2335−2338.
(14) Carlier, P. R.; Du, D.-M.; Han, Y.-F.; Liu, J.; Perola, E.; Williams, I. D.; Pang, Y.-P. Dimerization of an Inactive Fragment of Huperzine A Produces a Drug with Twice the Potency of the Natural Product. *Angew. Chem., Int. Ed. Engl.* **2000**, *39*, 1775−1777.
(15) Mary, A.; Renko, D. Z.; Guillou, C.; Thal, C. Potent Acetylcholinesterase Inhibitors: Design, Synthesis, and Structure−Activity Relationships of Bis-interacting Ligands in the Galanthamine Series. *Bioorg. Med. Chem.* **1998**, *6*, 1835−1850.
(16) Zeng, F.; Jiang, H.; Zhai, Y.; Zhang, H.; Chen, K.; Ji, R. Synthesis and Acetylcholinesterase Inhibitory Activity of Huperzine A−E2020 Combined Compound. *Bioorg. Med. Chem. Lett.* **1999**, *9*, 3279−3284.
(17) Camps, P.; El Achab, R.; Görbig, D. M.; Morral, J.; Muñoz-Torrero, D.; Badia, A.; Baños, J. E.; Vivas, N. M.; Barril, X.; Orozco, M.; Luque, F. J. Synthesis, in Vitro Pharmacology, and Molecular Modeling of Very Potent Tacrine-Huperzine A Hybrids as Acetylcholinesterase Inhibitors of Potential Interest for the Treatment of Alzheimer's Disease. *J. Med. Chem.* **1999**, *42*, 3227−3242.
(18) Barril, X.; Orozco, M.; Luque, F. J. Predicting Relative Free Energies of Tacrine-Huperzine A Hybrids as Inhibitors of Acetylcholinesterase. *J. Med. Chem.* **1999**, *42*, 5110−5119.
(19) Camps, P.; Contreras, J.; Font-Bardia. M.; Morral, J.; Muñoz-Torrero, D.; Solans, X. Enantioselective Synthesis of Tacrine-Huperzine A Hybrids. Preparative Chiral MPLC Separation of Their Racemic Mixtures and Absolute Configuration Assignments by X-ray Diffraction Analysis. *Tetrahedron: Asymmetry* **1998**, *9*, 835−849.
(20) Camps, P.; Cusack, B.; Mallender, W. D.; El Achab, R.; Morral, J.; Muñoz-Torrero, D.; Rosenberry, T. L. Huprine X is a Novel High-Affinity Inhibitor of Acetylcholinesterase That is of Interest for Treatment of Alzheimer's Disease. *Mol. Pharmacol.* **2000**, *57*, 409−417.
(21) Camps, P.; El Achab, R.; Font-Bardia. M.; Görbig, D. M.; Morral, J.; Muñoz-Torrero, D.; Solans, X.; Simon, M. Easy Synthesis of 7-Alkylbicyclo[3.3.1]non-6-en-3-ones by Silica Gel-Promoted Fragmentation of 3-Alkyl-2-oxaadamant-1-yl Mesylates. *Tetrahedron* **1996**, *52*, 5867−5880.
(22) Sepiol, J.; Mirek, J.; Soulen, R. L. Cyclization of Ylidene-Halodinitriles and Ylidenecyanoacetates Obtained from Mesityl Oxide and Pulegone. *Pol. J. Chem.* **1978**, *52*, 1389−1394.
(23) Hunziker, F.; Fischer, R.; Kipfer, P.; Schmutz, J.; Bürki, H. R.; Eichenberg, E.; White, T. G. Neuroleptic Piperazinyl Derivatives of 10*H*-Thieno[3,2-c][1]benzazepines and 4*H*-Thieno[2,3-c][1]-benzazepines. *Eur. J. Med. Chem.* **1981**, *16*, 391−398.
(24) Camps, P.; Morral, J.; Muñoz-Torrero, D. On the Synthesis of 2-Amino-4,6-difluorobenzonitrile: Highly Selective Formation of 5-Fluoro-3-nitro-1,2-benzoquinone 2-Diazide in the Attempted Sandmeyer Cyanation of 2,4-Difluoro-6-nitrobenzenediazonium Cation. *J. Chem. Res. (S)* **1998**, 144−145.
(25) Grivsky, E. M.; Hitchings, G. H. Synthesis of 2-Chloro-4-acetylaminobenzonitrile Isomeres. Structurally Related Compounds with Biological Activities. *Ind. Chim. Belge* **1974**, *39*, 490−500.
(26) Bogert, M. T.; Hoffman, A. Some Acyl Derivatives of Bromoanthranilic Nitrile, and the 7-Methyl-4-ketodihydroquinazolines Prepared Therefrom. *J. Am. Chem. Soc.* **1905**, *27*, 1293−1301.
(27) Beverung, Jr., W. N.; Partyka, A. Optionally Substituted 1,2,3,5-Tetrahydroimidazo[2,1-b]quinazolin-2-ones and 6*H*-1,2,3,4-Tetrahydropyrimido[2,1-b]quinazolin-2-ones. U.S. Patent 3.932.407, Bristol-Myers Co., 1976.
(28) Aguado, F.; Badia, A.; Baños, J. E.; Bosch, F.; Bozzo, C.; Camps, P.; Contreras, J.; Dierssen, M.; Escolano, C.; Görbig, D. M.; Muñoz-Torrero, D.; Pujol, M. D.; Simon, M.; Vázquez, M. T.; Vivas, N. M. Synthesis and Evaluation of Tacrine-Related Compounds for the Treatment of Alzheimer's Disease. *Eur. J. Med. Chem.* **1994**, *29*, 205−221.
(29) Badia, A.; Baños, J. E.; Camps, P.; Contreras, J.; Görbig, D. M.; Muñoz-Torrero, D.; Simon, M.; Vivas, N. M. Synthesis and Evaluation of Tacrine-Huperzine A Hybrids as Acetylcholinesterase Inhibitors of Potential Interest for the Treatment of Alzheimer's Disease. *Bioorg. Med. Chem.* **1998**, *6*, 427−440.
(30) Ellman, G. L.; Courtney, K. D.; Andres, B. Jr.; Featherstone, R. M. A New and Rapid Colorimetric Determination of Acetylcholinesterase Activity. *Biochem. Pharmacol.* **1961**, *7*, 88−95.
(31) Kawakami, H.; Ohuchi, R.; Kitano, M.; Ono, K. Quinoline Derivatives. Patent EPO 0 268 871 A1, Sumitomo Pharmaceuticals Co. Ltd., 1987.
(32) Benzi, G.; Moretti, A. Is there a Rationale for the Use of Acetylcholinesterase Inhibitors in the Therapy of Alzheimer's Disease? *Eur. J. Pharmacol.* **1998**, *346*, 1−13.
(33) Dixon, M.; Webb, E. C. *Enzymes*, 3rd ed.; Longman: London, 1979.
(34) Since the substrate concentration in the in vitro assays (performed at 298 K) was the same for all the inhibitors, the experimental differences in binding free energy can be derived from the competitive inhibition equation $IC_{50} = K_i(1 + [S]/K_m)$, where $K_m$ and $K_i$ are Michaelis and enzyme−inhibitor dissociation constants, respectively. The $IC_{50}$ value of (−)-**15** for AChE inhibition from bovine erythocytes is 47.1 ± 6.3 nM.[1]
(35) Baños, J. E.; Badia, A.; Jané, F. Facilitatory Action of Adrenergic Drugs on Muscle Twich Evoked by Nerve Stimulation in the Curarized Rat Phrenic-Hemidiaphragm. *Arch. Int. Pharmacodyn.* **1988**, *293*, 219−227.
(36) Riesz, M.; Kapati, E.; Szporni, L. Antagonism of Non-Depolarizing Neuromuscular Blockade by Aminopyridines in Cats. *J. Pharm. Pharmacol.* **1986**, *38*, 156−158.
(37) Wlodek, S. T.; Antosiewicz, J.; McCammon, J. A.; Straatsma, T. P.; Gilson, M. K.; Briggs, J. M.; Humblet, C.; Sussman, J. L. Binding of Tacrine and 6-Chlorotacrine by Acetylcholinesterase. *Biopolymers* **1996**, *38*, 109−117.
(38) Hariharan, P. C.; Pople, J. A. *Theoret. Chim. Acta* **1973**, *28*, 213-219.
(39) Frisch, M. J.; Trucks, G. W.; Schlegel, H. B.; Gill, P. M. W.; Johnson, B. G.; Robb, M. A.; Cheeseman, J. R.; Keith, T. A.; Petersson, G. A.; Montgomery, J. A.; Raghavachari, K.; Al-Laham, M. A.; Zakrzewski, V. G.; Ortiz, J. V.; Foresman, J. B.; Cioslowski, J.; Stefanov, B. B.; Nanayakkara, A.; Challacombe, M.; Peng, C. Y.; Ayala, P. Y.; Chen, W.; Wong, M. W.; Andres, J. L.; Replogle, E. S.; Gomperts, R.; Martin, R. L.; Fox, D. J.; Binkley, J. S.; Defrees, D. J.; Baker, J.; Stewart, J. P.; Head-Gordon, M.; Gonzalez, C.; Pople, J. A. *Gaussian 94*, revision A.1; Gaussian Inc.: Pittsburgh, PA, 1995.
(40) Jorgensen, W. L.; Chandrasekhar, J.; Madura, J. D.; Impey, R. W.; Klein, M. L. Comparison of Sample Potential Functions for Simulating Liquid Water. *J. Chem. Phys.* **1983**, *79*, 926−935.
(41) Pearlman, D. A. Determining the Contributions of Constraints in Free Energy Calculations: Development, Characterization, and Recommendations. *J. Chem. Phys.* **1993**, *98*, 8946−8957.
(42) Cornell, W. D.; Cieplak, P.; Bayly, C. I.; Gould, I. R.; Merz, K.; Ferguson, D. M.; Spellmeyer, D. C.; Fox, T.; Caldwell, J. W.; Kollman, P. A. Second Generation Force Field for the Simulation of Proteins, Nucleic Acids, and Organic Molecules. *J. Am. Chem. Soc.* **1995**, *117*, 5179−5197.
(43) Bayly, C. I.; Cieplak, P.; Cornell, W. D.; Kollman, P. A. A Well-Behaved Electrostatic Potential Based Method Using Charge Restraints for Deriving Atomic Charges. *J. Chem. Phys.* **1993**, *97*, 10269−10280.
(44) Jorgensen, W. L. *BOSS*, version 3.4; Yale University: New Haven, CT, 1990.
(45) Ryckaert, J. P.; Ciccotti, G.; Berendsen, H. J. C. Numerical Integration of the Cartesian Equations of Motion of a System with Constraints: Molecular Dynamics of *n*-Alkanes. *J. Comput. Phys.* **1977**, *23*, 327−341.
(46) Case, D. A.; Pearlman, D. A.; Caldwell, J. C.; Cheatham, T. E.; Ross, W. S.; Simmerling, C.; Darden, T.; Merz, K. M.; Stanton, R. V.; Cheng, A.; Vincent, J. J.; Crowley, M.; Ferguson, D. M.; Radmer, R.; Seibel, G. L.; Singh, U. C.; Weiner, P.; Kollman, P. A. *AMBER5*; University of California: San Francisco, CA, 1997.

JM000980Y